Nuclear Physics B312 (1989) 1–14
North-Holland, Amsterdam

NEUTRINO-COUNTING PROCESS ($e^+e^- \to \nu\bar{\nu}\gamma$) AND ITS MAJOR BACKGROUND ($e^+e^- \to e^+e^-\gamma$) AT THE Z^0 RESONANCE

H. VELTMAN

University of Michigan, Ann Arbor, MI 48109, USA

Received 10 December 1986
(Revised 6 May 1988)

The differential and the total cross sections for the neutrino-counting process ($e^+e^- \to \nu\bar{\nu}\gamma$) and its major source of background, radiative Bhabha scattering ($e^+e^- \to e^+e^-\gamma$), are calculated for some experimentally relevant kinematical regions, on and above the Z^0-resonance.

1. Introduction

There are two different ways currently being considered to find the number of neutrino generations. Either one can measure the width of the Z^0 or the cross section of $e^+e^- \to \nu\bar{\nu}\gamma$. Both of these measurements have their own problems and it will be very hard to determine accurately the number of neutrino families.

So far, experimental results from UA1 [1] seem to indicate that there are no more than ten types of neutrinos and from UA2 [2] the upper bound is seven.

Recently there has been much discussion [3–8] on neutrino counting using the process $e^+e^- \to \nu\bar{\nu}\gamma$ near the Z^0 resonance. Among the theoretical computations there seems to be some confusion about the numerical results from its background process $e^+e^- \to e^+e^-\gamma$. Here, both of these processes will be discussed. The method of calculation is very similar to ref. [6] and values of the experimental parameters used are most likely to be relevant for the SLC experiment [9].

This paper is organized as follows. In sect. 2 the expressions for the cross sections are derived and results will be presented for various values of the experimental parameters. Sect. 3 contains a discussion of the results and comparison with other calculations.

2. Computations of the cross-sections

In subsects. 2.1 and 2.2 the differential and the total cross sections will be computed and in subsect. 2.3 the numerical results will be presented. The kinematical region considered in detail will be that appropriate for the SLC experiment.

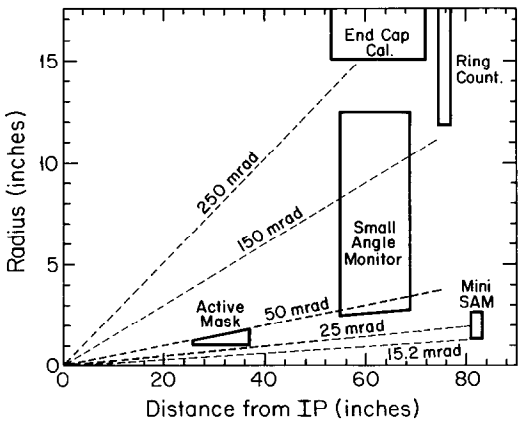

Fig. 1. Experimental setup at SLC (the mark II).

SLC is going to measure the process $e^+e^- \to \nu\bar{\nu}\gamma$ where only the photon is detected. Then it follows that $e^+e^- \to e^+e^-\gamma$ is a background process when the final electrons and positrons disappear down the beampipe. The Mark II at SLC can detect all electrons outside a cone whose axis is along the beam direction and whose half opening angle is 15 mrad. In order to reduce the background compared with the signal it is required that the photon-acceptance angle be large. For an illustration of the experimental setup at SLC see fig. 1.

The kinematics for the two processes are shown in fig. 2; p_1, p_2, k_1, q_1, q_2 are, respectively, the momenta of the incoming electron, the incoming positron, the outgoing photon, the outgoing electron or neutrino and the outgoing positron or anti-neutrino.

$\theta_1, \theta_2, \varphi_1, \varphi_2, \theta_\gamma$ are defined in fig. 2. With this notation the four-momentum vectors are chosen as follows (the electron masses are neglected)

$$p_1 = \begin{pmatrix} 0 \\ 0 \\ E \\ iE \end{pmatrix}, \qquad p_2 = \begin{pmatrix} 0 \\ 0 \\ -E \\ iE \end{pmatrix}, \qquad k = \begin{pmatrix} E_\gamma \sin\theta_\gamma \\ 0 \\ E_\gamma \cos\theta_\gamma \\ iE_\gamma \end{pmatrix},$$

$$q_1 = \begin{pmatrix} E_1 \sin\theta_1 \cos\varphi_1 \\ E_1 \sin\theta_1 \sin\varphi_1 \\ E_1 \cos\theta_1 \\ iE_1 \end{pmatrix}, \qquad q_2 = \begin{pmatrix} E_2 \sin\theta_2 \cos\varphi_2 \\ E_2 \sin\theta_2 \sin\varphi_2 \\ E_2 \cos\theta_2 \\ iE_2 \end{pmatrix}.$$

The following numerical values of the standard-model parameters have been taken

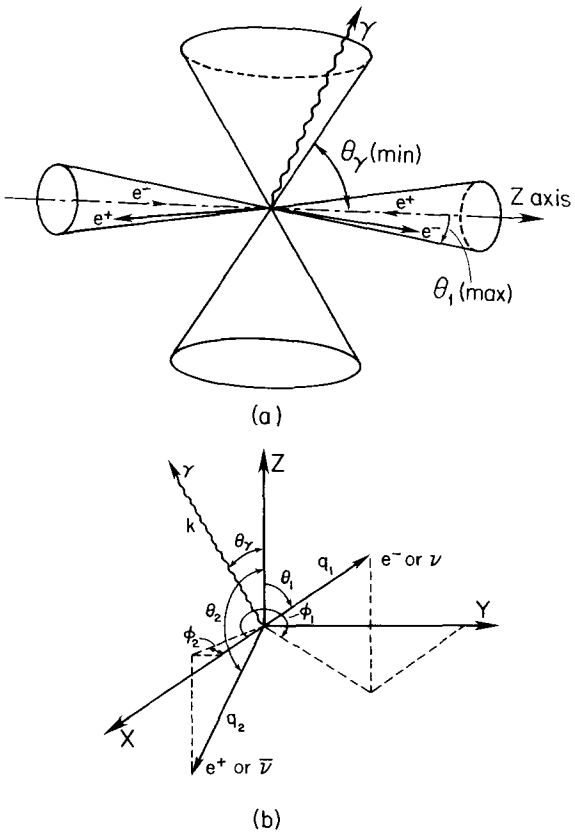

Fig. 2. Definition of the kinematics for $e^+e^- \to \nu\bar{\nu}\gamma$ and $e^+e^- \to e^+e^-\gamma$. The outgoing photon, electron and positron all lie in one plane.

for the calculations

$$\text{Fermi-coupling constant: } G_F = 1.16632 \times 10^{-5}\ \text{GeV}^{-1},$$

$$\text{Mass of the } Z^0\text{: } M_0 = 93.2\ \text{GeV},$$

$$\text{Width of the } Z^0\text{: } \Gamma_0 = 2.8\ \text{GeV} \quad \text{for} \quad N_\nu = 3,$$

$$\Gamma_0 = 2.98\ \text{GeV} \quad \text{for} \quad N_\nu = 4,$$

$$\text{Electroweak mixing angle } \theta_w\text{: } \sin^2\theta_w = 0.22$$

$$\text{Electromagnetic coupling constant: } \alpha = 1/137 \quad \text{for} \quad e^+e^- \to e^+e^-\gamma,$$

$$\alpha = 1/128.5 \quad \text{for} \quad e^+e^- \to \nu\bar{\nu}\gamma.$$

2.1. THE PROCESS $e^+e^- \to \nu\bar{\nu}\gamma$

The diagrams considered are shown in fig. 3. The matrix elements are

$$\langle S_1\rangle = \frac{1}{V^2}\frac{1}{\sqrt{2Vk_0}}(2\pi)^4 i \frac{1}{\left[(p_1+p_2-k)^2+M_0^2-iM_0\Gamma_0\right]}\left(\frac{ig}{4c_\theta}\right)^2(-ie)$$
$$\times\frac{1}{(p_1-k)^2}\left\{\bar{u}(q_1)\gamma^\mu(1+\gamma^5)u(-q_2)\right\}$$
$$\times\left\{\bar{u}(-p_2)\gamma^\mu(a+b\gamma^5)\left[-i(\not{p}_1-\not{k})\right]\not{\epsilon}_k u(p_1)\right\},$$

$$\langle S_2\rangle = \frac{1}{V^2}\frac{1}{\sqrt{2Vk_0}}(2\pi)^4 i \frac{1}{\left[(p_1+p_2-k)^2+M_0^2-iM_0\Gamma_0\right]}\left(\frac{ig}{4c_\theta}\right)^2(-ie)$$
$$\times\frac{1}{(p_2-k)^2}\left\{\bar{u}(q_1)\gamma^\mu(1+\gamma^5)u(-q_2)\right\}$$
$$\times\left\{\bar{u}(-p_2)\not{\epsilon}_k\left[+i(\not{p}_2-\not{k})\right]\gamma^\mu(a+b\gamma^5)u(p_1)\right\},$$

$$\langle S_3\rangle = \frac{1}{V^2}\frac{1}{\sqrt{2Vk_0}}(2\pi)^4 i \frac{1}{\left[(q_2-p_2)^2+M_w^2\right]}\left(\frac{ig}{2\sqrt{2}}\right)^2(-ie)$$
$$\times\frac{1}{(p_1-k)^2}\left\{\bar{u}(q_1)\gamma^\mu(1+\gamma^5)\left[-i(\not{p}_1-\not{k})\right]\not{\epsilon}_k u(p_1)\right\}$$
$$\times\left[\bar{u}(-p_2)\gamma^\mu(1+\gamma^5)u(-q_2)\right],$$

$$\langle S_4\rangle = \frac{1}{V^2}\frac{1}{\sqrt{2Vk_0}}(2\pi)^4 i \frac{1}{\left[(q_1-p_1)^2+M_w^2\right]}\left(\frac{ig}{2\sqrt{2}}\right)^2(-ie)$$
$$\times\frac{1}{(p_2-k)^2}\left\{\bar{u}(q_1)\gamma^\mu(1+\gamma^5)u(p_1)\right\}$$
$$\times\left\{\bar{u}(-p_2)\not{\epsilon}_k\left[+i(\not{p}_2-\not{k})\right]\gamma^\mu(1+\gamma^5)u(-q_2)\right\},$$

where

$$\frac{g^2}{(4c_\theta)^2}=\frac{G_F M_0^2}{2\sqrt{2}}, \qquad \frac{g^2}{8}=\frac{G_F M_w^2}{\sqrt{2}},$$

$$a=2g_v=4\sin^2\theta_w-1, \qquad b=2g_A=-1,$$

$$\langle S\rangle=\langle S_1\rangle+\langle S_2\rangle-\langle S_3\rangle-\langle S_4\rangle.$$

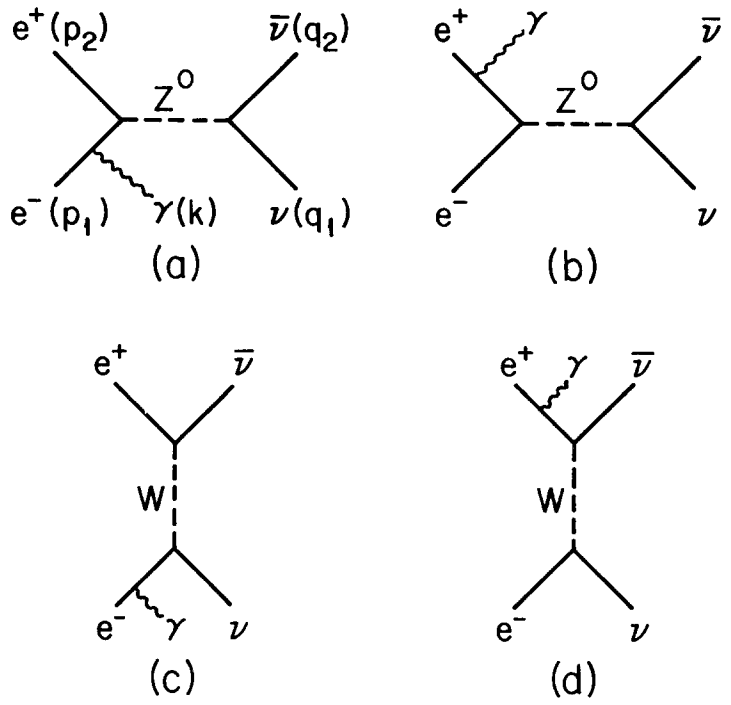

Fig. 3. The diagrams considered for $e^+e^- \to \nu\bar{\nu}\gamma$.

The total unpolarized cross-section is by definition

$$\sigma_{\text{tot}} = \frac{V}{(2\pi)^3}\int d_3k \frac{V}{(2\pi)^3}\int d_3q_1 \frac{V}{(2\pi)^3}\int d_3q_2 \frac{VT}{(2\pi)^4}\delta_4(p_1+p_2-k-q_1-q_2)$$

$$\times\left(\frac{V}{2T}\right)\overline{|\langle S\rangle|^2}; \tag{1}$$

$\overline{|\langle S\rangle|^2}$ was evaluated using SCHOONSCHIP [10]. It follows that the differential cross section is given by [4]

$$\frac{d^2\sigma}{d\cos\theta\, dx} = \frac{G_F^2\alpha}{6\pi^2}\left\{\frac{M_0^4\left(N_\nu\left(g_v^2+g_A^2\right)+2\left(g_v+g_A\right)\left[1-s(1-x)/M_0^2\right]\right)}{\left[s(1-x)-M_0^2\right]^2+M_0^2\Gamma_0^2}+2\right\}$$

$$\times\frac{s}{x(1-\cos^2\theta)}\left[(1-x)\left(1-\tfrac{1}{2}x\right)^2+\tfrac{1}{4}x^2(1-x)\cos^2\theta\right]; \tag{2}$$

here $\alpha = 1/128.5$ and $x = E_\gamma/E$, where E is the beam energy of the incoming electrons and positrons.

The total cross section can easily be calculated analytically. The final expressions are somewhat lengthy and will not be explicitly written down.

2.2. THE PROCESS $e^+e^- \to e^+e^-\gamma$

Here there are sixteen diagrams in the lowest order (see fig. 4). In the kinematical region of interest only the t-channel diagrams with virtual photon exchange are important. In fact all the other twelve diagrams give a negligible contribution as has been explicitly checked ($\ll 1\%$).

In the following all eight photon-propagator (s- and t-channel) diagrams will be taken into consideration. (In this case the expression for the differential cross section is nice and compact.) The matrix elements are (for the first eight diagrams in fig. 4)

$$\langle S_1\rangle = \frac{1}{V^2}\frac{1}{\sqrt{2Vk_0}}\frac{(2\pi)^4 ie^3}{2(q_1q_2)}\left\{\bar{u}(-p_2)\not{\epsilon}_1\frac{[-(\not{p}_2-\not{k})]}{-2(p_2k)}\gamma^\mu u(p_1)\right\}[\bar{u}(q_1)\gamma^\mu u(-q_2)],$$

$$\langle S_2\rangle = \frac{1}{V^2}\frac{1}{\sqrt{2Vk_0}}\frac{(2\pi)^4 ie^3}{2(q_1q_2)}\left\{\bar{u}(-p_2)\gamma^\mu\frac{[+(\not{p}_1-\not{k})]}{-2(p_1k)}\not{\epsilon}_1 u(p_1)\right\}[\bar{u}(q_1)\gamma^\mu u(-q_2)],$$

$$\langle S_3\rangle = \frac{1}{V^2}\frac{1}{\sqrt{2Vk_0}}\frac{(2\pi)^4 ie^3}{2(p_1p_2)}[\bar{u}(-p_2)\gamma^\mu u(p_1)]\left\{\bar{u}(q_1)\gamma^\mu\frac{[-(\not{q}_2+\not{k})]}{2(q_2k)}\not{\epsilon}_2 u(-q_2)\right\},$$

$$\langle S_4\rangle = \frac{1}{V^2}\frac{1}{\sqrt{2Vk_0}}\frac{(2\pi)^4 ie^3}{2(p_1p_2)}[\bar{u}(-p_2)\gamma^\mu u(p_1)]\left\{\bar{u}(q_1)\not{\epsilon}_2\frac{[+(\not{q}_1+\not{k})]}{2(q_1k)}\gamma^\mu u(-q_2)\right\},$$

$$\langle S_5\rangle = \frac{1}{V^2}\frac{1}{\sqrt{2Vk_0}}\frac{(2\pi)^4 ie^3}{-2(p_1q_1)}\left\{\bar{u}(-p_2)\not{\epsilon}_4\frac{[-(\not{p}_2-\not{k})]}{-2(p_2k)}\gamma^\mu u(-q_2)\right\}[\bar{u}(q_1)\gamma^\mu u(p_1)],$$

$$\langle S_6\rangle = \frac{1}{V^2}\frac{1}{\sqrt{2Vk_0}}\frac{(2\pi)^4 ie^3}{-2(p_2q_2)}[\bar{u}(-p_2)\gamma^\mu u(-q_2)]\left\{\bar{u}(q_1)\gamma^\mu\frac{[(\not{p}_1-\not{k})]}{-2(p_1k)}\not{\epsilon}_3 u(p_1)\right\},$$

$$\langle S_7\rangle = \frac{1}{V^2}\frac{1}{\sqrt{2Vk_0}}\frac{(2\pi)^4 ie^3}{-2(p_1q_1)}\left\{\bar{u}(-p_2)\gamma^\mu\frac{[-(\not{q}_2+\not{k})]}{2(q_2k)}\not{\epsilon}_4 u(-q_2)\right\}[\bar{u}(q_1)\gamma^\mu u(p_1)],$$

$$\langle S_8\rangle = \frac{1}{V^2}\frac{1}{\sqrt{2Vk_0}}\frac{(2\pi)^4 ie^3}{-2(p_2q_2)}[\bar{u}(-p_2)\gamma^\mu u(-q_2)]\left\{\bar{u}(q_1)\not{\epsilon}_3\frac{[(\not{q}_1+\not{k})]}{2(q_1k)}\gamma^\mu u(p_1)\right\},$$

$$\langle S\rangle = \langle S_1\rangle + \langle S_2\rangle + \langle S_3\rangle + \langle S_4\rangle - \langle S_5\rangle - \langle S_6\rangle - \langle S_7\rangle - \langle S_8\rangle;$$

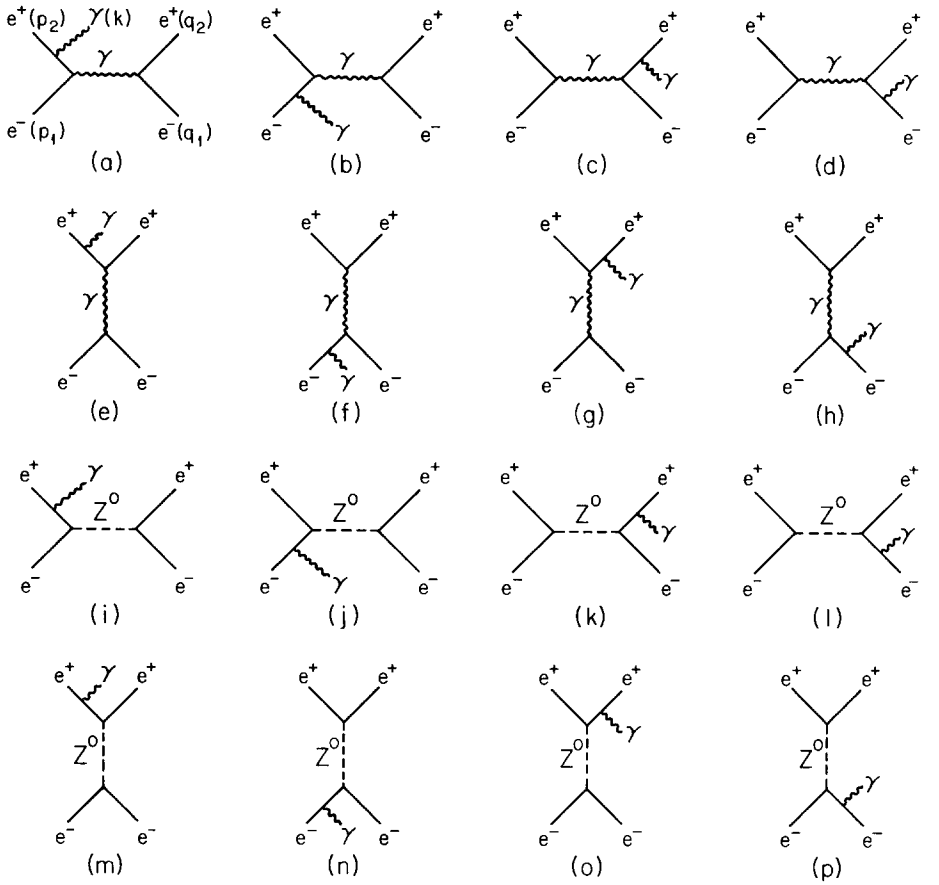

Fig. 4. The diagrams relevant for $e^+e^- \to e^+e^-\gamma$.

using the polarization method [11] one ends up with [12]

$$\overline{|\langle S\rangle|^2} = \frac{1}{2V^5}\,\frac{1}{k_0 p_{10} q_{10} q_{20}}\,\frac{(2\pi)^8}{16}$$

$$\times \frac{\left(-e^6(v_q - v_p)^2\right)}{ss'tt'}\left[ss'(s^2+s'^2)+tt'(t^2+t'^2)+uu'(u^2+u'^2)\right], \quad (3)$$

where

$$v_q = \frac{q_2}{(q_2k)} - \frac{q_1}{(q_1k)} \quad \text{and} \quad v_p = \frac{p_2}{(p_2k)} - \frac{p_1}{(p_1k)}$$

and the total cross section is given by eq. (1). This expression has been checked by using the standard method with SCHOONSCHIP.

Since the angle between the photon and the outgoing electron and positron is always large, one may, in the first approximation, neglect the masses of the electron and positron in the numerator in eq. (3). But still one has to be very careful with t and t' in the denominator, since they can get extremely small and the masses cannot be neglected in this case. For clarity these have been written as t_ϕ and t'_ϕ in order to distinguish them from the t and t' in the numerator in eq. (3).

Thus, the kinematic invariants are defined as

$$s = 2(p_1p_2), \qquad s' = 2(q_1q_2),$$

$$t = -2(p_2q_2), \qquad t' = -2(p_1q_1),$$

$$u = -2(p_2q_1), \qquad xu' = -2(p_1q_2),$$

$$t_\phi = 2\{p_m q_{2m}\cos\theta_2 + EE_2\} - 2m^2,$$

$$t'_\phi = -2\{p_m q_{1m}\cos\theta_1 - EE_1\} - 2m^2,$$

where

$$p_m = \sqrt{E^2 - m^2},$$

$$q_{1m} = \sqrt{E_1^2 - m^2}, \qquad q_{2m} = \sqrt{E_2^2 - m^2}.$$

Also

$$(p_1k) = \tfrac{1}{2}(s + t' + u'), \qquad (p_2k) = \tfrac{1}{2}(s + t + u),$$

$$(q_1k) = -\tfrac{1}{2}(s' + u + t') = \tfrac{1}{2}(s + u' + t),$$

$$(q_2k) = -\tfrac{1}{2}(s' + u' + t) = \tfrac{1}{2}(s + u + t'),$$

(since $s + s' + t + t' + u + u' = 0$). Besides low-momentum transfer there logically is also a low scattering angle. Therefore the cosine in t_ϕ and t'_ϕ can be expanded in a Taylor series

$$\cos x = 1 - \tfrac{1}{2}x^2\left[1 - \tfrac{1}{12}x^2\left(1 - \tfrac{1}{30}x^2\right)\right] \ldots .$$

The cross section can be written as

$$\sigma_{\text{tot}} = \frac{\alpha^3}{(2\pi)}\int \mathrm{d}E_\gamma\,\mathrm{d}\cos\theta_\gamma\,\mathrm{d}\cos\theta_1\,\mathrm{d}\varphi_1\,\frac{E_1^2E_\gamma}{ss'}(v_q - v_p)^2$$

$$\times\frac{1}{ss't_\phi t'_\phi}\left[ss'(s^2 + s'^2) + tt'(t^2 + t'^2) + uu'(u^2 + u'^2)\right], \tag{4}$$

where

$$(v_q - v_p)^2 = \left[\frac{-s'}{(q_1k)(q_2k)} + \frac{-s}{(p_1k)(p_2k)} + \frac{+t}{(p_2k)(q_2k)} + \frac{+t'}{(p_1k)(q_1k)} + \frac{-u}{(p_2k)(q_1k)} + \frac{-u'}{(p_1k)(q_2k)} \right],$$

$$E_1 = \frac{2E^2 - 2EE_\gamma}{\left(2E - E_\gamma + E_\gamma(\sin\theta_\gamma \sin\theta_1 \cos\varphi_1 + \cos\theta_1 \cos\theta_\gamma)\right)}.$$

There are four integration variables left. The integrations were numerically evaluated using the program RIWIAD [13].

2.3. NUMERICAL RESULTS

The results of this analysis are presented in tables 1 and 2 and figs. 5 and 6.

Table 1 gives the total cross sections for $e^+e^- \to \nu\bar{\nu}\gamma$ and $e^+e^- \to e^+e^-\gamma$ for the number of neutrino generations $N_\nu = 3, 4$. The range of values for θ_1 and θ_γ has been taken as

$$0 < \theta_1(\text{electron}) < 15 \text{ mrad},$$

$$20° < \theta_\gamma(\text{photon}) < 160°.$$

Table 2 is the same as table 1 but in this case

$$30° < \theta_\gamma < 150°.$$

These parameters are relevant for the SLC (see fig. 1). Initially, SLC will start running at the Z^0-resonance (93 GeV) and measure photons down to an angle of 30° with respect to the beam axis, but later runs at higher energies are planned and photons will be measured down to 20°.

The cross sections are given in picobarn (pb) in an energy range between 93 and 98 GeV.

Figs. 5 and 6 give the corresponding spectra of $d\sigma/dE_\gamma$ versus E_γ. These show how the total signal will look when there are three neutrino generations compared with when there are four.

3. Discussion

Here, to begin with, some of the tests of the integration program that have been carried out will be briefly described and then the results obtained in this paper will be compared with other calculations.

TABLE 1
Total cross sections for: $e^+e^- \to \nu\bar{\nu}\gamma$, $N_\nu = 3$ (row 1); $e^+e^- \to \nu\bar{\nu}\gamma$, $N_\nu = 4$ (row 2); and $e^+e^- \to e^+e^-\gamma$ (row 3) $0 < \theta_1 < 15$ mrad and $20° < \theta_\gamma < 60°$, E and E_γ in GeV, cross sections in picobarns (pb)

E_γ/E	93	94	95	96	97	98
	80.3	119.2	80.0	41.7	23.9	15.4
0.5–1.0	98.6	140.4	97.6	52.5	30.4	19.6
	80.0	78.9	77.0	76.5	75.1	73.9
	47.1	93.5	110.0	66.9	35.5	20.9
1.0–2.0	60.0	112.8	130.4	82.2	44.8	26.6
	39.2	39.4	39.3	39.7	39.7	39.8
	13.1	26.1	52.2	63.6	39.4	20.9
2.0–3.0	17.3	33.3	63.1	75.3	48.4	26.6
	0.43	0.5	0.5	0.5	0.5	0.6
	5.0	8.9	17.6	35.4	44.5	28.2
3.0–4.0	6.8	11.7	22.5	42.9	52.7	34.5
	–	–	–	–	–	–
	2.4	3.7	6.5	12.9	26.2	34.0
4.0–5.0	3.2	5.0	8.7	16.5	31.8	40.3
	–	–	–	–	–	–
	1.2	1.8	2.9	5.1	9.9	20.2
5.0–6.0	1.7	2.5	3.9	6.7	12.7	24.7
	–	–	–	–	–	–
	0.7	1.0	1.5	2.3	4.0	7.8
6.0–7.0	1.0	1.4	2.0	3.1	5.3	10.1
	–	–	–	–	–	–
	–	0.6	0.8	1.2	1.9	3.3
7.0–8.0	–	0.8	1.1	1.7	2.6	4.3
	–	–	–	–	–	–
	–	–	–	0.7	1.0	1.6
8.0–9.0	–	–	–	1.0	1.4	2.1
	–	–	–	–	–	–

As a first test, only the s-channel diagrams ((a)–(d), (i)–(l) in fig. 4) were put in and as expected, the weak contribution completely dominates over the QED contribution at the Z^0-resonance. Next, it was explicitly checked that the term in the spin-averaged matrix-element squared that is proportional to the $\epsilon_{\mu\nu\rho\gamma}$ tensor does not contribute to the total cross section. This is because of time-reversal invariance.

After completion of the work, ref. [8] was received. Their results have been checked and they were found to be in complete agreement. In an earlier paper, ref. [6], the value of α was chosen to be $1/128.5$ for both the processes, rather than

TABLE 2
Same as table 1 except the minimum photon angle is taken to be $30° < \theta_\gamma < 150°$

E_γ/E	93	94	95	96	97	98
	61.0	90.5	60.7	31.7	10.1	11.7
0.5–1.0	74.8	106.6	74.0	39.9	23.1	14.8
	29.7	29.3	29.3	29.1	28.3	27.9
	35.8	71.0	83.5	50.7	26.9	15.9
1.0–2.0	45.5	85.6	98.9	62.4	34.0	20.2
	4.7	5.2	5.2	5.3	5.5	5.8
	9.9	19.8	39.6	48.2	29.9	15.8
2.0–3.0	13.1	25.3	47.9	57.12	38.7	20.0
	–	–	–	–	–	–
	3.8	6.7	13.4	26.9	33.8	21.4
3.0–4.0	5.15	8.9	17.1	32.6	39.96	26.2
	–	–	–	–	–	–
	1.8	2.8	5.0	9.8	19.9	25.8
4.0–5.0	2.43	3.82	6.56	12.53	24.1	30.54
	–	–	–	–	–	–
	1.0	1.4	2.2	3.8	7.5	5.4
5.0–6.0	1.3	1.9	3.0	5.1	9.6	18.7
	–	–	–	–	–	–
	–	0.8	1.1	1.8	3.1	5.9
6.0–7.0	–	1.0	1.5	2.4	4.0	7.6
	–	–	–	–	–	–
	–	–	0.6	0.9	1.4	2.5
7.0–8.0	–	–	0.9	1.3	1.9	3.2
	–	–	–	–	–	–
	–	–	–	–	1.0	1.6
8.0–9.0	–	–	–	–	1.1	1.6
	–	–	–	–	–	–

1/137 for $e^+e^- \to e^+e^-\gamma$ and 1/128.5 for $e^+e^- \to \nu\bar{\nu}\gamma$, as is done in this work. This results in an overestimation of the cross sections for the background process by about 20%. This may have been part of the disagreement with ref. [7].

Finally, we conclude with a remark concerning the effect of the higher order radiative corrections to the processes considered. Part of these, some of the logarithmic ones, have been incorporated in the process $e^+e^- \to \nu\bar{\nu}\gamma$ by using the value of the running QED coupling at the Z^0 mass. i.e. $\alpha = 1/128.5$. In the same approximation, since small-momentum transfers are only relevant for $e^+e^- \to e^+e^-\gamma$,

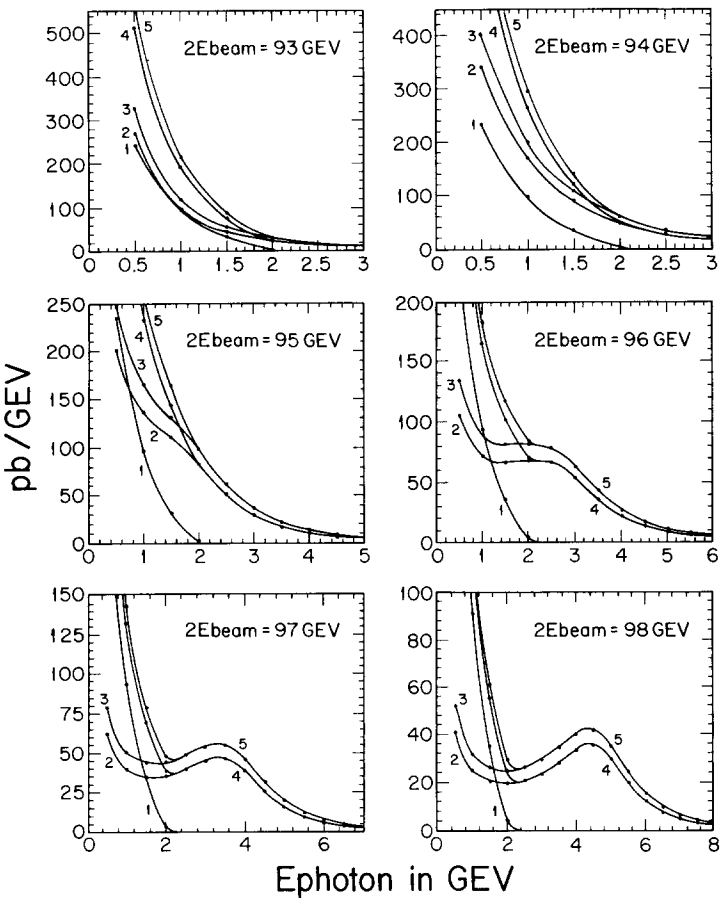

Fig. 5. $d\sigma/dE_\gamma$ versus E_γ where $0 < \theta_1 < 15$ mrad, $20° < \theta_\gamma < 160°$, for 5 different cases in each plot: line 1 – background; line 2 – $e^+e^- \to \nu\bar{\nu}$, $N_\nu = 3$; line 3 – $e^+e^- \to \nu\bar{\nu}$, $N_\nu = 4$; line 4 – resulting signal for $N_\nu = 3$ (line 1 added to line 2); and line 5 – resulting signal for $N_\nu = 4$ (line 1 added to line 3).

the value of α taken here is 1/137. At this point it is worth emphasizing that it is quite clear that two of the α's in $e^+e^- \to \nu\bar{\nu}\gamma$ should be taken to the 1/128.5, however, it is not apparent that the third α, which results from non-collinear bremsstrahlung, should be also taken at this value. In fact, this α is no different from the corresponding α in $e^+e^- \to e^+e^-\gamma$ which arises from the non-collinear bremsstrahlung and perhaps for consistency should be also put to 1/137. This would change the numerical results presented for $e^+e^- \to \nu\bar{\nu}\gamma$ by a few percent. Moreover, by using the value of the running QED coupling at Z^0 mass for the cross section $e^+e^- \to \nu\bar{\nu}\gamma$ we do not claim to completely incorporate the leading logs in this cross section but merely some of the higher order logarithmic corrections. Further, as is well-known [14], sometimes the constant terms, coming from a

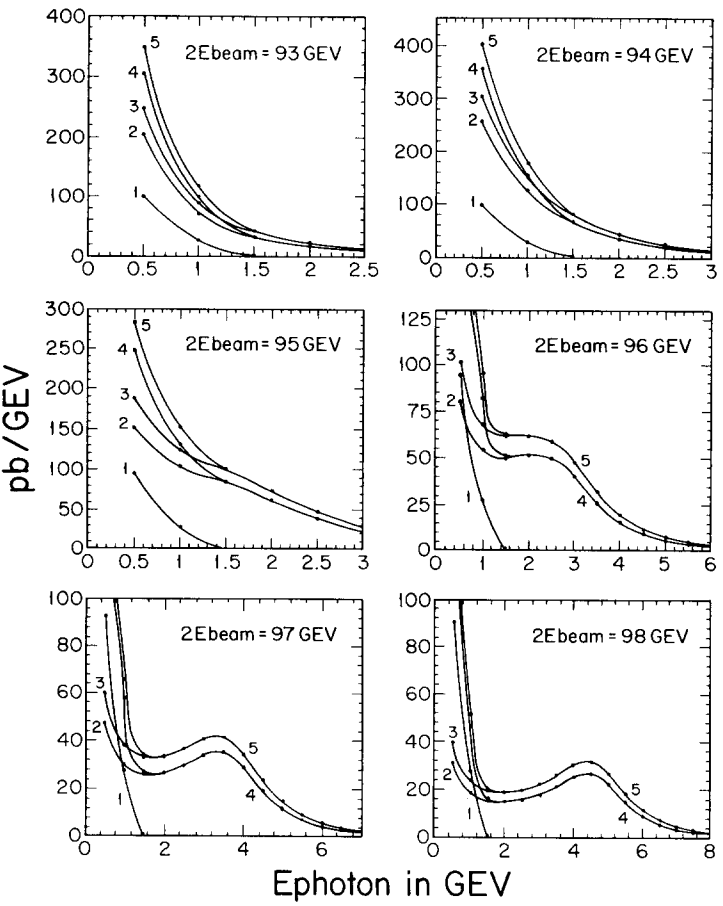

Fig. 6. The same as fig. 5 but here $30° < \theta_\gamma < 150°$.

complete analysis of the radiative corrections, are of the same order of magnitude as the logarithmic ones. In view of these remarks, the numerical results presented should be considered reliable within about 20% only. To do better, the complete radiative corrections to the processes considered here will have to be systematically evaluated.

The author would like to thank G. Passarino for suggesting this problem. The author is grateful to R. Akhoury for his invaluable help and assistance during all stages of the project. We are grateful to the referee for his remarks on the choice of the QED coupling constants. This work was supported in part by the US Department of Energy.

References

[1] G. Arnison et al., preprint CERN-EP/85-160
[2] J.A. Appel et al., preprint CERN-EP/85-166
[3] E. Ma and J. Okada, Phys. Rev. Lett. 41 (1978) 287
[4] K.J.F. Gaemers, R. Gastmans and R.M. Renard, Phys. Rev. Lett. D19 (1979) 1605
[5] B. Richter and J.L. Siegrist, Phys. Lett., B106 (1981) 414
[6] M. Caffo, R. Gatto and E. Remiddi, Phys. Lett., B173 (1986) 91
[7] C. Mana and M. Martinez, preprint DESY 86-062, G. Bonvicinni, private communication
[8] M. Caffo, R. Gatto and E. Remiddi, UGVA-DPT (1986) 109
[9] R. Thun, private communication
[10] M. Veltman, private communication
[11] P. de Causmaecker, R. Gastmans and W. Troost, Nucl. Phys. B206 (1982) 53
[12] F.A. Berends, R. Kleiss, P. de Causmaecker, R. Gastmans, W. Troost and T.T. Wu, Nucl. Phys B206 (1982) 61
[13] B. Lautrup, RIWIAD, CERN-DD report D114
[14] M. Veltman, Phys. Lett. B91 (1980) 95